

UNCLASSIFIED

AD 296 364

*Reproduced
by the*

**ARMED SERVICES TECHNICAL INFORMATION AGENCY
ARLINGTON HALL STATION
ARLINGTON 12, VIRGINIA**



UNCLASSIFIED

NOTICE: When government or other drawings, specifications or other data are used for any purpose other than in connection with a definitely related government procurement operation, the U. S. Government thereby incurs no responsibility, nor any obligation whatsoever; and the fact that the Government may have formulated, furnished, or in any way supplied the said drawings, specifications, or other data is not to be regarded by implication or otherwise as in any manner licensing the holder or any other person or corporation, or conveying any rights or permission to manufacture, use or sell any patented invention that may in any way be related thereto.

296 364

CATALOGED BY ASTIA
AS AD NO.

296364

RADC-TDR-62-363



A STUDY OF THE WIRE-GRID LENS

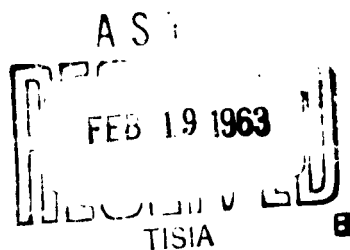
TECHNICAL DOCUMENTARY REPORT NO. RADC-TDR-62-363
(TRG-West Project W-101 TDR No. 1)

July 1962

Prepared for

Rome Air Development Center
Air Force Systems Command
Griffiss Air Force Base, New York

(Prepared under Contract AF 30(602)-2742, FSC-0082
by M. G. Andreasen of TRG-West, A Division of TRG
Inc., 153 University Ave, Palo Alto, Calif.)



Qualified requestors may obtain copies of this report from the ASTIA Document Service Center, Arlington Hall Station, Arlington 12, Virginia. ASTIA Services for the Department of Defense contractors are available through the "Field of Interest Register" on a "need-to-know" certified by the cognizant military agency of their project or contract.

When US Government drawings, specifications, or other data are used for any purpose other than a definitely related government procurement operation, the government thereby incurs no responsibility nor any obligation whatsoever; and the fact that the government may have formulated, furnished, or in any way supplied the said drawings, specifications, or other data is not to be regarded by implication or otherwise, as in any manner licensing the holder or any other person or corporation, or conveying any rights or permission to manufacture, use, or sell any patented invention that may in any way be related thereto.

Do not return this copy. Retain or destroy.

ABSTRACT

This report presents a study of some of the problems that are of importance in the design of a wire-grid lens of the circularly symmetric type.

The first problem investigated is that of a double-wire square-mesh grid which will very often be used near the rim of the lens to keep the grid-to-grid spacing suitably small. Design formulas for the quasi-static equivalent dielectric constant of such grids have been derived. The validity of these formulas was tested experimentally.

Another problem that was investigated is that of synthesizing the index of refraction in a circularly symmetric lens when the index of refraction is specified in part of the lens and when it is required that the rays leaving the lens must form a collimated beam in as large an aperture as possible. Design formulas representing the solution of this problem have been derived. These formulas are most useful for wire-grid lens designs because the grid-to-grid spacing in the outer part of the lens is often determined by mechanical considerations rather than by electrical considerations.

PUBLICATION REVIEW

This report has been reviewed and is approved.

Approved:

Edward N. Munzer
EDWARD N. MUNZER
Chief, Electronic Warfare Laboratory
Directorate of Intelligence & Electronic Warfare

Approved:

Robert J. Quinn
ROBERT J. QUINN, JR., Col, USAF
Director of Intelligence & Electronic Warfare

CONTENTS

| | Page |
|------------------------------|--|
| Abstract | i |
| List of Illustrations | v |
| | |
| 1. | INTRODUCTION |
| 2. | DOUBLE-WIRE SQUARE-MESH GRIDS |
| 3. | CIRCULARLY SYMMETRIC LENS WITH PARTIALLY PRESCRIBED INDEX |
| 3.1 | General |
| 3.2 | The Rays in the Lens |
| 3.3 | Synthesis of Lens |
| 4. | CONCLUSIONS |
| | |
| Appendix A | 40 |
| References | 42 |

ILLUSTRATIONS

| | Page |
|---|-------------|
| Fig. 1 Double-Wire Grid | 5 |
| Fig. 2 Single Cell of a Pair of Double-Wire Grids | 8 |
| Fig. 3 Transformation of Grid Cell in Complex Plane | 9 |
| Fig. 4 Equivalent Static Dielectric Constant of a Pair of Double-Wire Grids $b/r_o = 200$ | 18 |
| Fig. 5 Ray w Path in a Circularly Symmetric Lens | 21 |
| Fig. 6 Possible nr-Distributions in a Circularly Symmetric Lens | 26 |
| Fig. 7 Ray w Paths in a Lens with an nr-Distribution as shown in Fig. 6B | 28 |
| Fig. 8 Example of Circularly Symmetric Wire-Grid Lens | 35 |
| Fig. 9 w-H-Product for Example in Fig. 8 | 36 |
| Fig. 10 The e Index of Refraction for Example in Fig. 8 | 37 |

1. INTRODUCTION

In recent years, there has been a need for scanning directional antennas which can be used in the HF frequency band (3 - 30 Mc) for direction-finding applications. Artificial dielectrics practical and economical at these frequencies have not existed, however. A most important structure, which makes possible lens designs in the HF band, is a pair of wire grids with either square, hexagonal or triangular meshes. A pair of wire grids can be used for lens designs because the velocity of a wave propagating between the grids can be controlled by changing the ratio between the grid spacing and the mesh size. The wire-grid lens as a direction-finding antenna and problems related to the design of such antennas is the subject of investigation in this report.

A great number of problems have to be solved to realize a wire-grid lens. Part of these problems have already been solved previously through support by the United States Air Force under Contracts AF 19(604)-2240 and AF 19(604)-8059.^{1, 2, 3} The work on these contracts was carried out at Stanford Research Institute and included a determination of the equivalent static dielectric constant of a pair of grids with square, hexagonal and triangular mesh in relation to the grid dimensions. Also investigated were the dynamic properties of a pair of grids by an experimental method. The usefulness of the results obtained was demonstrated by testing an experimental model of a wire-grid lens designed according to the developed design information.

While the investigations of the wire-grid lens undertaken at Stanford Research Institute led to important basic data needed in a practical design, many problems yet have to be solved before a practical wire-grid lens can be realized. Among these problems are:

- (1) An extended theoretical investigation of the dispersion and anisotropy of a pair of parallel wire grids
- (2) An investigation of grid structures whose equivalent dielectric constant can be controlled continuously, not only by changing the grid spacing but also by changing the mesh structure; for example, by changing the effective mesh size
- (3) An investigation of various radiating structures to provide the required matching between the lens and free space
- (4) An investigation of various feed structures
- (5) An investigation of circularly symmetric lenses whose dielectric constant can be specified in part of the lens
- (6) An investigation of the radiation pattern of a wire-grid lens including the effect of dispersion and anisotropy.

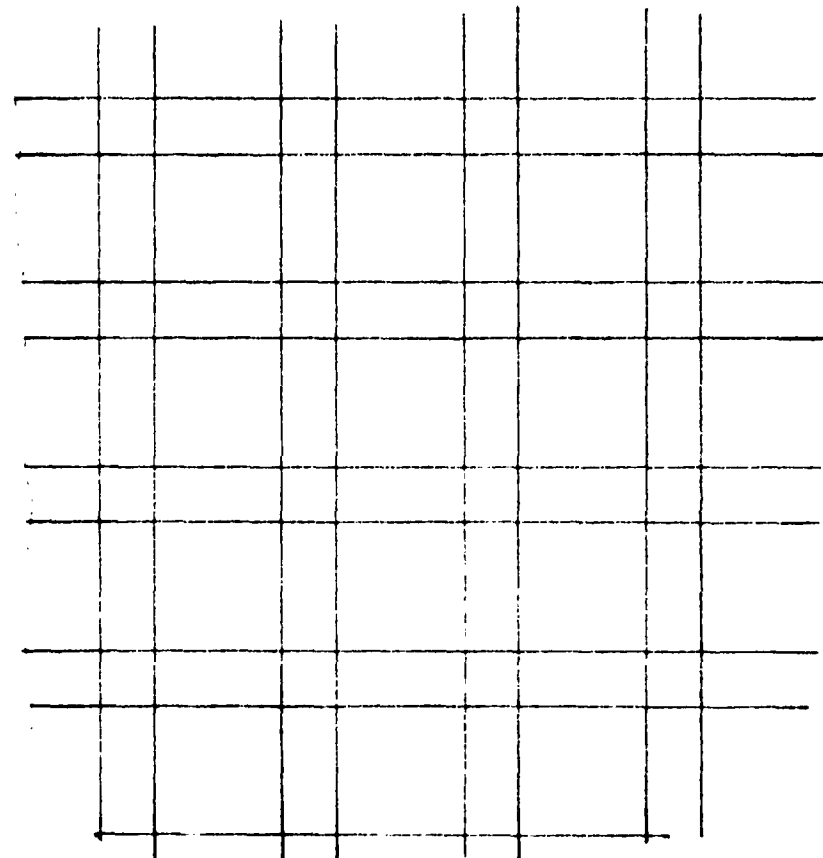
In this report, problems (2) and (5) are treated.

In one of the reports³ referred to above, square-mesh, hexagonal-mesh and triangular-mesh grids were investigated. As a result of the investigation, it was found that, for the same mesh area, hexagonal-mesh grids exhibit

less anisotropy and dispersion than both square-mesh grids and triangular-mesh grids. From an economical point of view, however, the square mesh will most often be superior to the hexagonal mesh because a square-mesh grid is much simpler to construct than a hexagonal-mesh grid. In this report, therefore, only square-mesh grids are investigated.

2. DOUBLE-WIRE SQUARE-MESH GRIDS

The equivalent dielectric constant of a pair of square-mesh grids is a function of the ratio between the grid spacing and the mesh size. The smaller this ratio, the larger the dielectric constant. For very closely spaced grids, the dielectric constant approaches 2 while it approaches 1 for grids that are far apart relative to the mesh size. At the rim of a circularly symmetric wire-grid lens, it is usually necessary that the equivalent dielectric constant be close to the value 1. This requires the spacing between the grids to be very large near the rim of the lens. In many cases, the required spacing between the rim of the lens turns out to be larger than practically desirable. To illustrate this, assume that a dielectric constant of 1.1 is desired at the rim of the lens. For a square-mesh grid lens with a constant mesh size of 5 feet, which would be a reasonable mesh size for an HF lens, it is then necessary to use a spacing of about 35 feet. This spacing could be reduced by a factor of between 2 and 3 by reducing the mesh size by a factor of 2. However, reducing the mesh size by a factor of 2 increases the cost of the lens by nearly a factor of 2 and is therefore not a practical solution. A practical solution to the problem was proposed by Dr. R. L. Tanner, TRG-West, prior to the contract period; by using a double-wire square-mesh grid, (see Fig. 1) with varying spacing d between the wires of the double-wire near the rim of the lens, the effective mesh size can be reduced by a factor of 2 near the rim of the lens while keeping the mesh size unchanged in the larger part of the lens.



- d -

- b -

Wire radius : r_0
Grid spacing : $2a$

Fig. 1 Double-Wire Grid

In this section, formulas will be derived for the equivalent dielectric constant of a pair of double-wire square-mesh grids in dependence of the ratio between the grid spacing and the mesh size, and of the wire radius and of the spacing between the wires of the double wire. This represents the basic information needed for designing a pair of double-wire square-mesh grids. The dielectric constant will be derived by a method analogous to the method which was previously used to evaluate the dielectric constant of a pair of single-wire square-mesh grids.¹

The equivalent static dielectric constant can be expressed as the ratio between the capacitance per cell of the grids, and the capacitance per cell of the grids with one set of parallel wires removed. The capacitance will be calculated from the variational expression

$$C = \frac{(\int \rho dl)^2}{\int \rho \phi dl} \quad (1)$$

where ρ is the charge stored per unit length of the wires, and ϕ is the electrostatic potential produced at the wire surface. When ρ is the correct charge distribution, ϕ is constant along the wires. Otherwise, ϕ changes on the wire surface. However, since Eq. (1) is stationary with respect to small changes of ρ , this equation can provide a reasonably accurate expression for C even if ρ is not too close to the correct distribution. Since the capacitance can be easily evaluated for a constant charge density on the wires, and this charge distribution should be reasonably accurate except near the points where wires intersect each other (where the charge density drops to a lower

value) we shall now assume that the charge is uniformly distributed on the wires.

For a constant charge density we can take advantage of the fact that the electrostatic field in a cell is a sum of two dimensional fields. Accordingly, we can use the theory of complex functions to find the potential of the line charges in the cell.

A single cell of the grids is shown in Fig. 2. A cross section of this cell is shown in Fig. 3A. $y = 0$ and $y = b$ are magnetic walls at which the normal derivative of the electrostatic potential has to be zero. Consider first the potential produced by the line charges parallel to the z -axis. Assuming the xy -plane to be a complex z -plane ($z = x + iy$), transform the strip $0 < y < b$ to the upper half of a ζ -plane by the transformation

$$\zeta = e^{\frac{z}{b}\pi} \quad (2)$$

The magnetic walls $y = 0$ and $y = b$ thereby transform to the real axis of the ζ -plane. The positions of the line charges transform as follows

$$z_{1+} = a + i \frac{b-d}{2} \quad \longrightarrow \quad \zeta_{1+} = e^{\frac{a}{b}\pi} e^{i\frac{\pi}{2}(1-\frac{d}{b})} \quad (3)$$

$$z_{2+} = a + i \frac{b+d}{2} \quad \longrightarrow \quad \zeta_{2+} = e^{\frac{a}{b}\pi} e^{i\frac{\pi}{2}(1+\frac{d}{b})} \quad (4)$$

$$z_{1-} = -a + i \frac{b-d}{2} \quad \longrightarrow \quad \zeta_{1-} = e^{-\frac{a}{b}\pi} e^{i\frac{\pi}{2}(1-\frac{d}{b})} \quad (5)$$

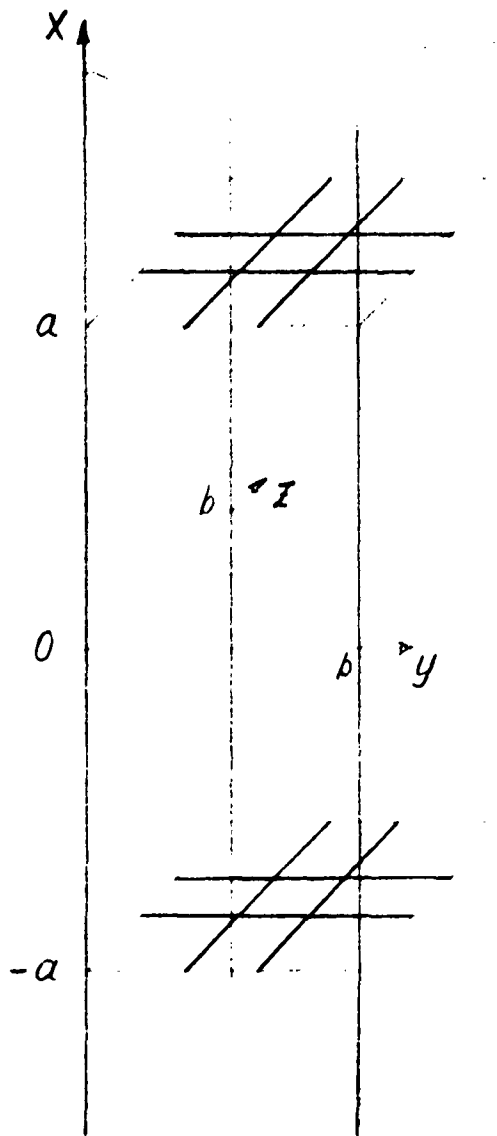
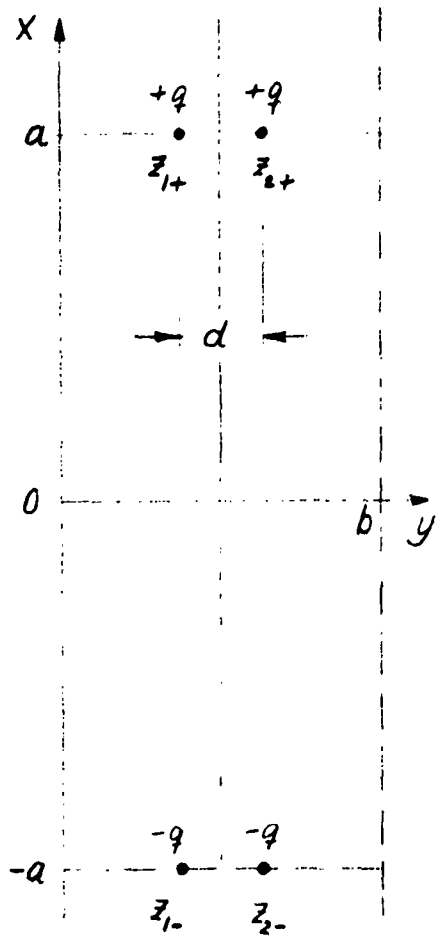
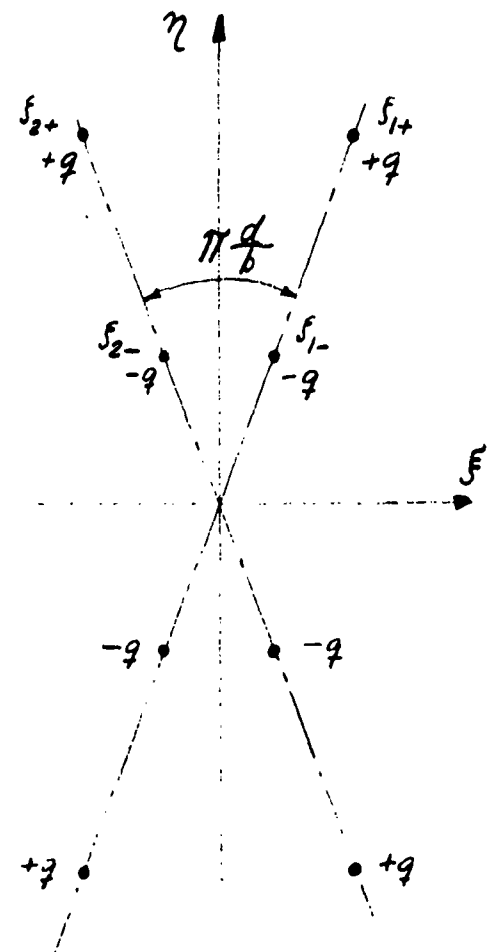


Fig. 2 Single Cell of a Pair of Double-Wire Grids



z -plane
A



s -plane
B

Fig. 3 Transformation of Grid Cell in Complex Plane

$$z_{2-} = -a + i \frac{b+d}{2} \quad \longrightarrow \quad f_{2-} = e^{-\frac{a}{b}\pi} e^{i \frac{\pi}{2}(1-\frac{d}{b})} \quad (6)$$

The positions are marked in Fig. 3. Imaging the four line charges in the upper half of the ζ -plane in the ξ -axis, the system of charges shown in Fig. 3B is obtained.

Assuming that the charge per unit length of the wires is q , the complex potential in the ζ -plane is found to be

$$\Phi = -\frac{q}{2\pi\epsilon_0} \ln \left[\frac{(f^2 - f_{1+}^2)(f^2 - f_{2+}^2)}{(f^2 - f_{1-}^2)(f^2 - f_{2-}^2)} \right] \quad (7)$$

where ϵ_0 is the dielectric constant of the medium.

The real potential ϕ_0 in the z -plane is the real part of Φ . Introducing Eq. (2) above, we find then

$$\phi_0 = -\frac{q}{2\pi\epsilon_0} \ln \left| \frac{\left(1 + e^{\frac{a-z}{b}2\pi - i\frac{d}{b}\pi}\right)\left(1 + e^{\frac{a-z}{b}2\pi + i\frac{d}{b}\pi}\right)}{\left(1 + e^{-\frac{a+z}{b}2\pi - i\frac{d}{b}\pi}\right)\left(1 + e^{-\frac{a+z}{b}2\pi + i\frac{d}{b}\pi}\right)} \right| \quad (8)$$

The potential at the plane $x = 0$ mid between the grids (this is an electric plane because of symmetry) is found from this expression to be

$$\varphi_{\text{ground}} = -\frac{q}{\epsilon_0} \frac{2a}{b} \quad (9)$$

We want the potential at $x = 0$ to be zero. This can be achieved by subtracting Eq. (9) from Eq. (8). Doing so, we find

$$\varphi_0 = -\frac{q}{2\pi\epsilon_0} \ln \left| \frac{\left(1 + e^{\frac{a-z}{b}2\pi - i\frac{d}{b}\pi}\right)\left(1 + e^{\frac{a-z}{b}2\pi + i\frac{d}{b}\pi}\right)}{\left(1 + e^{-\frac{a+z}{b}2\pi - i\frac{d}{b}\pi}\right)\left(1 + e^{-\frac{a+z}{b}2\pi + i\frac{d}{b}\pi}\right)} e^{-\frac{a}{b}4\pi} \right| \quad (10)$$

To evaluate the capacitance according to Eq. (1), we need to know the electrostatic potential at the wire surface, this is, at a distance r_0 from the points z_{1+} or z_{2+} . According to Eq. (10), this potential is very nearly constant and equals

$$\varphi_0 = \frac{q}{2\pi\epsilon_0} \left\{ \ln\left(\frac{b}{\pi r_0}\right) + \ln \sinh\left(\frac{a}{b}2\pi\right) - \frac{1}{2} \ln \left[\frac{1 - \cos\left(\frac{d}{b}2\pi\right)}{\cosh\left(\frac{a}{b}4\pi\right) - \cos\left(\frac{d}{b}2\pi\right)} \right] \right\} \quad (11)$$

The total charge on two parallel wires in a cell of the double-wire grids is $2 qb$. The capacitance of one set of parallel wires, introducing Eq. (11) in Eq. (1), therefore is

$$C_0 = \frac{qb}{\phi_0} = \frac{2\pi\epsilon_0 b}{\ln \left[\frac{b}{\pi r_0} \sinh \left(\frac{a}{b} 2\pi \right) \right] \sqrt{\frac{\cosh \left(\frac{a}{b} 4\pi \right) - \cos \left(\frac{a}{b} 2\pi \right)}{1 - \cos \left(\frac{a}{b} 2\pi \right)}}} \quad (12)$$

The capacitance of one grid cell with both sets of parallel wires in place can be expressed as

$$C_1 = \frac{qb^2}{\int \varphi dl} \quad (13)$$

where the integration is extended over one-half the length of one of the wires carrying the charge q per unit length. The potential ϕ equals the sum of the above constant potential ϕ_0 (see Eq. (11)) and a varying potential ϕ_1 which is produced by the charge on the set of wires perpendicular to the set of wires producing the constant potential ϕ_0 . Equation (13) reduces to

$$C_1 = \frac{qb^2}{\phi_0 \frac{b}{2} + \int \varphi dl} \quad (14)$$

ϕ_1 is evaluated along the line $z = a - r_0 + iy$ (see Fig. 3). Introducing this value of z in Eq. (8), we find

$$\phi_1 = -\frac{q}{2\pi\epsilon_0} \ln \left| \frac{\left(1+e^{\frac{r_0}{b}2\pi-i\frac{y+\frac{q}{2}}{b}2\pi}\right)\left(1+e^{\frac{r_0}{b}2\pi-i\frac{y-\frac{q}{2}}{b}2\pi}\right)e^{-\frac{q}{b}4\pi}}{\left(1+e^{-\frac{2a-r_0}{b}2\pi-i\frac{y+\frac{q}{2}}{b}2\pi}\right)\left(1+e^{-\frac{2a-r_0}{b}2\pi-i\frac{y-\frac{q}{2}}{b}2\pi}\right)} \right| \quad (15)$$

This can be reduced to

$$\begin{aligned} \phi_1 = & -\frac{q}{4\pi\epsilon_0} \left\{ \frac{r_0}{b}4\pi + \ln \left[\cosh \left(\frac{r_0}{b}2\pi \right) + \cos \left(\frac{y+\frac{q}{2}}{b}2\pi \right) \right] \right. \\ & + \ln \left[\cosh \left(\frac{r_0}{b}2\pi \right) + \cos \left(\frac{y-\frac{q}{2}}{b}2\pi \right) \right] \\ & - \ln \left[\cosh \left(\frac{2a-r_0}{b}2\pi \right) + \cos \left(\frac{y+\frac{q}{2}}{b}2\pi \right) \right] \\ & \left. - \ln \left[\cosh \left(\frac{2a-r_0}{b}2\pi \right) + \cos \left(\frac{y-\frac{q}{2}}{b}2\pi \right) \right] \right\} \end{aligned} \quad (16)$$

When this expression is integrated over y from $y = 0$ to $y = \frac{b}{2}$, we find

$$\int \varphi_i dl = \frac{q}{\epsilon_0} (a - r_o) \quad (17)$$

Introducing this in Eq. (14), the following expression is found for the capacitance of a single cell of a double-wire grid.

$$C_i = \frac{4\pi\epsilon_0 b}{4\pi \frac{a-r_o}{b} + \ln \left[\frac{b}{\pi r_o} \sinh \left(\frac{a}{b} 2\pi \right) \right] \sqrt{\frac{\cosh \left(\frac{a}{b} 4\pi \right) - \cos \left(\frac{d}{b} 2\pi \right)}{1 - \cos \left(\frac{d}{b} 2\pi \right)}}} \quad (18)$$

The equivalent static dielectric constant of a pair of double-wire square-mesh grids is therefore given by the following expression.

$$\epsilon = \frac{C_i}{C_0} = 2 \frac{G}{G + 4\pi \frac{a-r_o}{b}} \quad (19)$$

where G is defined by

$$G = \ln \left[\frac{b}{\pi \epsilon_0} \sinh \left(\frac{a}{b} 2\pi \right) \right] \sqrt{\frac{\cosh \left(\frac{a}{b} 4\pi \right) - \cos \left(\frac{d}{b} 2\pi \right)}{1 - \cos \left(\frac{d}{b} 2\pi \right)}} \quad (20)$$

It is easily seen from Eq. (19) that $\epsilon \rightarrow 2$ for $\frac{a}{b} \rightarrow 0$, and that $\epsilon \rightarrow 1$ for $\frac{a}{b} \rightarrow \infty$. This was, of course, expected.

The accuracy of Eq. (19) is reasonably good despite the fact that the assumption of a constant charge density on the wires may not be very good close to the points where the grid wires intersect. Yet it may be important to improve the accuracy of Eq. (19) by considering a charge distribution that approximates the correct charge distribution better than the constant charge density. The mathematically simplest charge distribution which will give an improvement of Eq. (19) is a constant charge density plus a point charge placed in each intersection point. The optimum amount of charge to be placed in each intersection point is such as to make the capacitance expression stationary with respect to a change of this charge. The calculation of the improved capacitance is lengthy and trivial and shall be excluded from this report. It suffices to mention that the potential of the point charge was found by expanding the potential in mode functions of the grid cell. As a result of the calculation, the improved dielectric constant was found to be expressed by

$$\epsilon_{impr} = \epsilon \frac{1+2\alpha+\alpha^2}{1+a_1\alpha+a_2\alpha^2} \quad (21)$$

where ϵ is the dielectric constant defined in Eq. (19), and α is related to the functions a_1 and a_2 by

$$\alpha = -\frac{a_1 - 2}{2a_2 - a_1} \quad (22)$$

while a_1 and a_2 are related to the grid dimensions and to the function G (Eq. 20) as follows

$$a_1 = \frac{4G}{G + 4\pi \frac{a}{b}} \quad (23)$$

and

$$a_2 = \frac{1}{2} \frac{\frac{b}{T_0} + \frac{b}{a} \left(2 + \frac{1}{12} \right) + 16\pi \frac{a}{b}}{G + 4\pi \frac{a}{b}} \quad (24)$$

Equation (21) has been plotted in Fig. 4 which shows ϵ as a function of $\frac{a}{b}$ for various values of $\frac{d}{b}$, and for $\frac{b}{r_0} = 200$ which value is close to the value used in the experiments described below.

To test the validity of Eq. (21), experimental measurements were made using a rectangular resonator operating in the TE_{omn} modes in which the top wall of the resonator was replaced by the wire grid. The method of determining the grid dielectric constant from the resonant frequencies of the resonator was described in a previous report.¹ The agreement between theory and experiment was excellent. For a grid resonator with the parameters $\frac{a}{b} = 0.251$, $\frac{d}{b} = 0.124$ and $\frac{b}{r_0} = 230$, a value of 1.405 was measured for the equivalent dielectric constant. The theoretical value predicted by Fig. 4 is 1.395. For another grid resonator described by the parameters $\frac{a}{b} = 0.6$, $\frac{d}{b} = 0.124$ and $\frac{b}{r_0} = 230$, a value of 1.21 was measured for ϵ . The theoretical value is 1.213 according to Fig. 4. It can, therefore, be concluded that the accuracy of Eq. (21) is very good. Equation (21) was programmed as a sub-routine for an electronic computer. This sub-routine will be used in subsequent computations on wire-grid lenses.

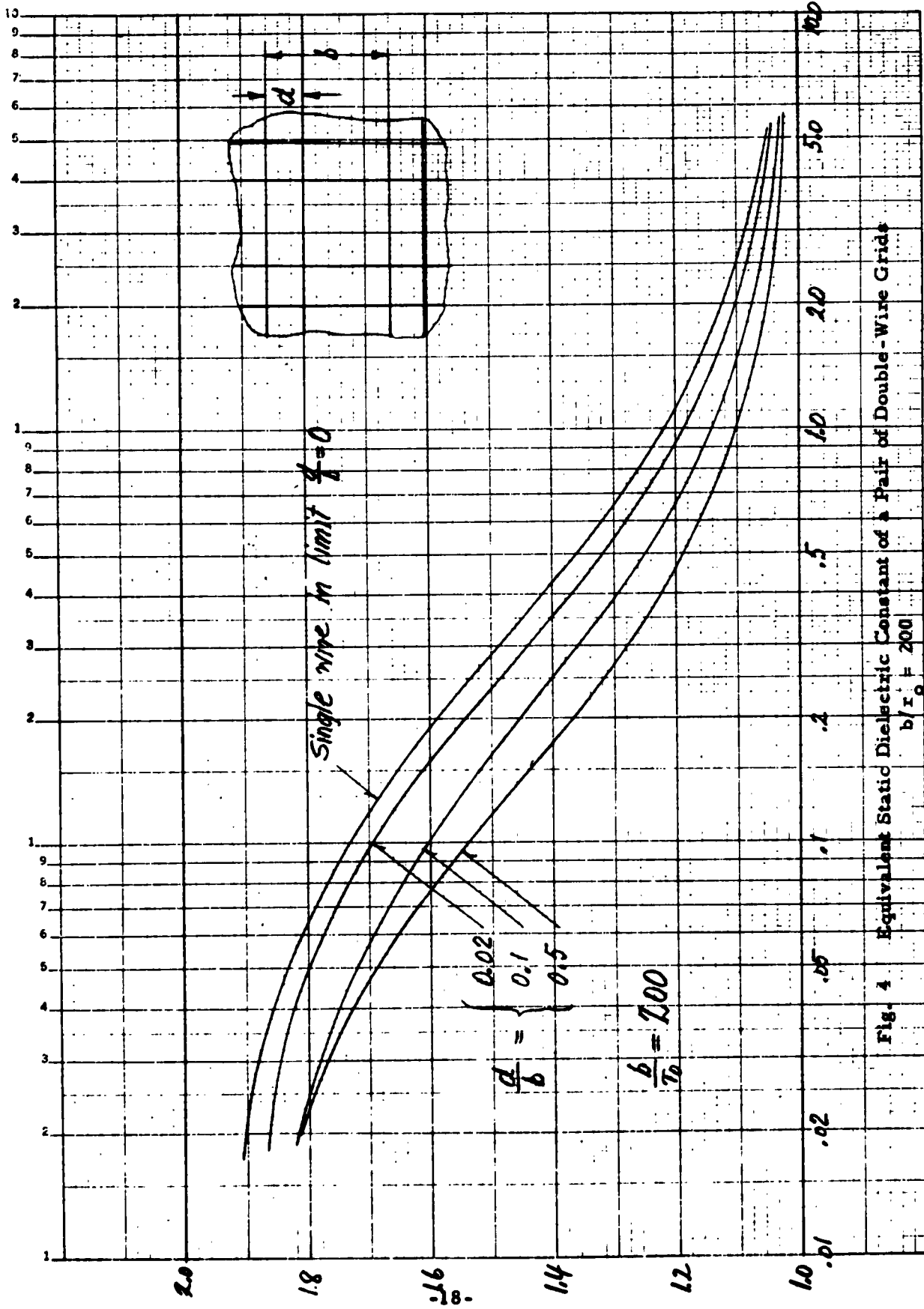


Fig. 4 Equivalent Static Dielectric Constant of a Pair of Double-Wire Grids
 $b/r_0 = 200$

3. CIRCULARLY SYMMETRIC LENS WITH PARTIALLY PRESCRIBED INDEX

3.1 General

For many applications of a circularly symmetric lens using an artificial dielectric for the lens material, the variation of refractive index required for a Luneburg Lens is not practical. In particular, a maximum index of refraction less than $\sqrt{2}$ is desirable for a wire-grid lens. One method by which the maximum index of refraction required to collimate the rays leaving the front part of the lens (opposite to the feed) can be made less than $\sqrt{2}$ is to place the feed a certain distance away from the rim of the lens. The lens with the displaced feed can be considered a rim-fed lens whose index of refraction has been assigned the value 1 in an outer ring.

In practice, the index of refraction in the outer part of a circularly symmetric lens will often be determined by mechanical considerations more than by electrical considerations, and it may not be possible to produce any prescribed variation of the index of refraction. In view of this and in view of the above considerations concerning the maximum index of refraction, a practical design requires the solution of the general problem of synthesizing a lens whose index of refraction is specified in an outer ring and which is fed by a point source somewhere in this ring. The purpose of the investigation in this section is to pursue this problem.

3.2 The Rays in the Lens

A cross section of one-half of a spherically-symmetric lens and the path of a ray through this lens is shown in Fig. 5. The index of refraction is specified in the ring $r_a < r < r_c$. The point-source feed is placed at a distance r_f from the lens center, $r_a < r_f < r_c$. We want to determine the index of refraction in the inner core of the lens ($r < r_a$) such that the rays leaving the front part of the lens (opposite to the feed) are collimated in as large an aperture as possible. To do so, we shall first establish the general relation between the radially varying index of refraction $n(r)$, the ray angle ψ and the angle ψ_o of the turning point, that is, that point of the ray which is closest to the center of the lens (see Fig. 5).

The rays in the lens move along paths obeying Snell's law which can be written

$$n r \sin \nu = \chi \quad (25)$$

where χ is a constant characteristic of the particular ray. χ is different for different rays and is related to the ray angle ψ as follows

$$\chi = n_f r_f \sin \psi \quad (26)$$

where n_f is the index of refraction at the point where the feed is placed. χ may also be related to the index of refraction n_o and radius r_o at the turning point as follows.

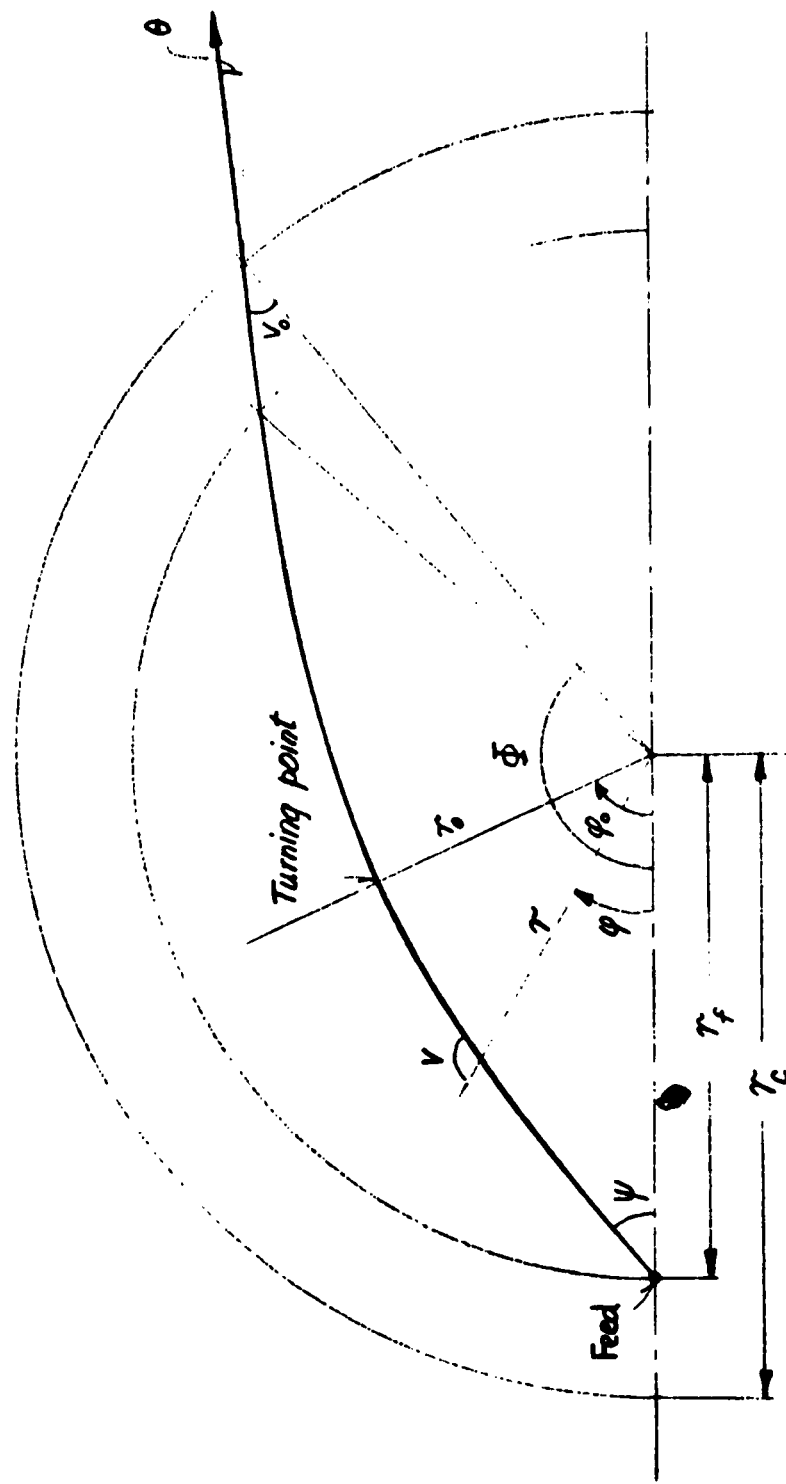


Fig. 5 Ray Path in a Circularly Symmetric Lens

$$\chi = n_o r_o \quad (27)$$

The polar angle of the turning point is most easily found by considering the differential form of Snell's law

$$\frac{n r^2 \frac{d\phi}{dr}}{\sqrt{1 + \left(r \frac{d\phi}{dr}\right)^2}} = \pm \chi \quad (28)$$

where the upper sign is used when the ray approaches the turning point while the lower sign is used when the ray recedes away from the turning point.

When Eq. (28) is solved with respect to $\frac{d\phi}{dr}$, we find

$$\frac{d\phi}{dr} = \pm \frac{\chi}{r \sqrt{n^2 r^2 - \chi^2}} \quad (29)$$

Integrating with respect to r , we find the following expression for the polar angle ϕ

$$\phi = \chi \int_r^{r_f} \frac{dr}{r \sqrt{n^2 r^2 - \chi^2}} \quad (30)$$

when the ray is approaching the turning point. When the ray is receding from the turning point, the following expression should be used for ϕ

$$\varphi = \varphi_0(x) + x \int_{r_0}^r \frac{dr}{r \sqrt{n^2 r^2 - x^2}} \quad (31)$$

where φ_0 is the polar angle of the turning point

$$\varphi_0(x) = x \int_{r_0}^{r_f} \frac{dr}{r \sqrt{n^2 r^2 - x^2}} \quad (32)$$

According to Eq. (31), the polar angle Φ of the point where the ray leaves the lens is

$$\Phi = 2\varphi_0(x) + x \int_{r_f}^{r_c} \frac{dr}{r \sqrt{n^2 r^2 - x^2}} \quad (33)$$

The angle θ between the direction of the ray after leaving the lens and the principal direction of the lens according to Eq. (25) and Fig. 5 is defined by the relation

$$r_c \sin [\pi - (\Phi + \theta)] = x \quad (34)$$

from which it follows that

$$\theta = \pi - \phi - \arcsin\left(\frac{x}{r_c}\right) \quad (35)$$

The above formulas are useful for determining ray paths when the index of refraction is specified throughout the lens. These formulas form the basis for synthesizing a lens whose index of refraction is unknown in part of the lens and for calculating radiation patterns.

3.3 Synthesis of Lens

We shall now consider the synthesis problem: given the index of refraction for $r_a < r < r_c$, to find the index in the inner region $0 < r < r_a$ such that those rays that pass through the inner region form a collimated beam in as large an aperture as possible upon leaving the lens. To solve this problem, consider Eq. (32). This is an integral equation from which the index n can be found when ϕ_o is given as a function of χ . According to Eq. (26), ϕ_o is defined in the range $0 < \chi < n_f r_f$. A certain part of this range belongs to rays that do not penetrate the inner region $0 < r < r_a$ of the lens. The value of $\phi_o(\chi)$ in this part of the total range of χ can be calculated from the given index of refraction for $r > r_a$ by Eq. (32). However, some care has to be exercised in the use of Eq. (32) if n_r is not a monotonic function of r .

If n_r is a monotonic function of r (see Fig. 6A), Eq. (32) can be used with no difficulties. The rays that do not penetrate the inner region $0 < r < r_a$ of the lens are in that case those for which χ has a value in the range $n_a r_a < \chi < n_f r_f$. Physically, the monotonic variation of n_r with r implies that one, and always one, ray passes through every point in the lens.

Assume now that n_r is not a monotonic function of r , as in the examples with two extrema of the rn -curve shown in Figs. 6B and 6C. In these figures, r'' is the radius for which n_r assumes the minimum while $r' < r''$ is the radius for which n_r has the same value as for $r = r''$.

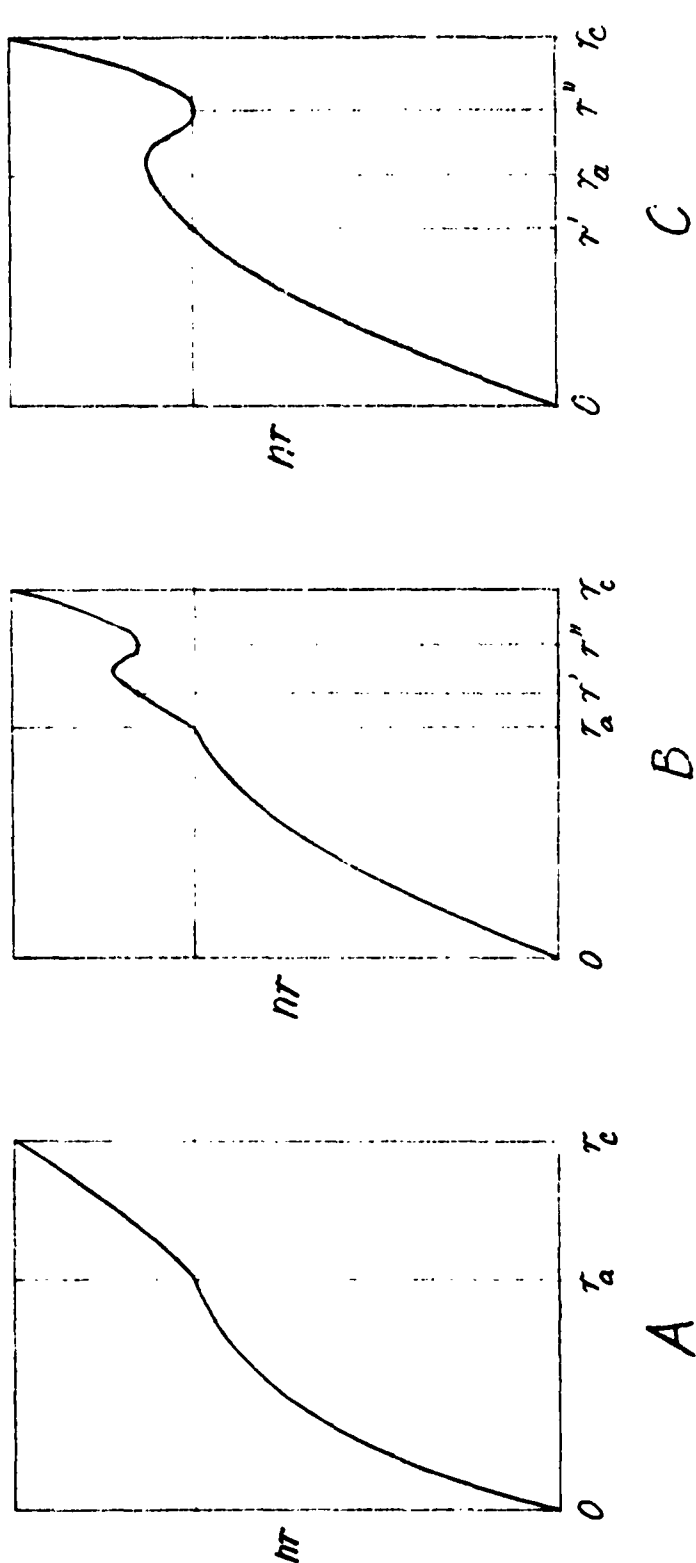


Fig. 6 Possible nr -Distributions in a Circularly Symmetric Lens

Consider first Fig. 6B where $n_a r_a$ is the lowest value of nr for $r > r_a$. In that case r_o in Eq. (32) cannot be allowed to have any value in the range from r_a to r_f , but the interval $r' < r_o < r''$ must be excluded from that range. Since $r_a < r' < r''$, the rays that do not penetrate the inner region $0 < r < r_a$ of the lens are again those for which χ has a value in the range $n_a r_a < \chi < n_f r_f$. The physical consequence of the type of variation of nr shown in Fig. 6B is that a ray will not pass through any point of the lens. This is illustrated in Fig. 7. This variation is seen to have the effect of producing regions of "darkness" in the lens. This may be a desirable feature for many applications.

In Fig. 6C where $r' < r_a < r''$, the rays that do not penetrate the inner region $0 < r < r_a$ of the lens are those for which χ has a value in the range $n''r'' < \chi < n_f r_f$. In contrast to the nr -curves in Figs. 6A and 6B, the nr -curve in Fig. 6C is not allowed because it makes it impossible to determine the refraction index in the region $0 < r < r_a$. To solve Eq. (32) for the index of refraction in the inner part of the lens from a prescribed variation of ϕ_o with χ for the rays that penetrate the inner part of the lens, assume that $n_a r_a$ is the smallest value of nr for $r > r_a$. The range of χ for the rays penetrating the region $0 < r < r_a$ is therefore

$$0 < \chi < n_a r_a \quad (36)$$

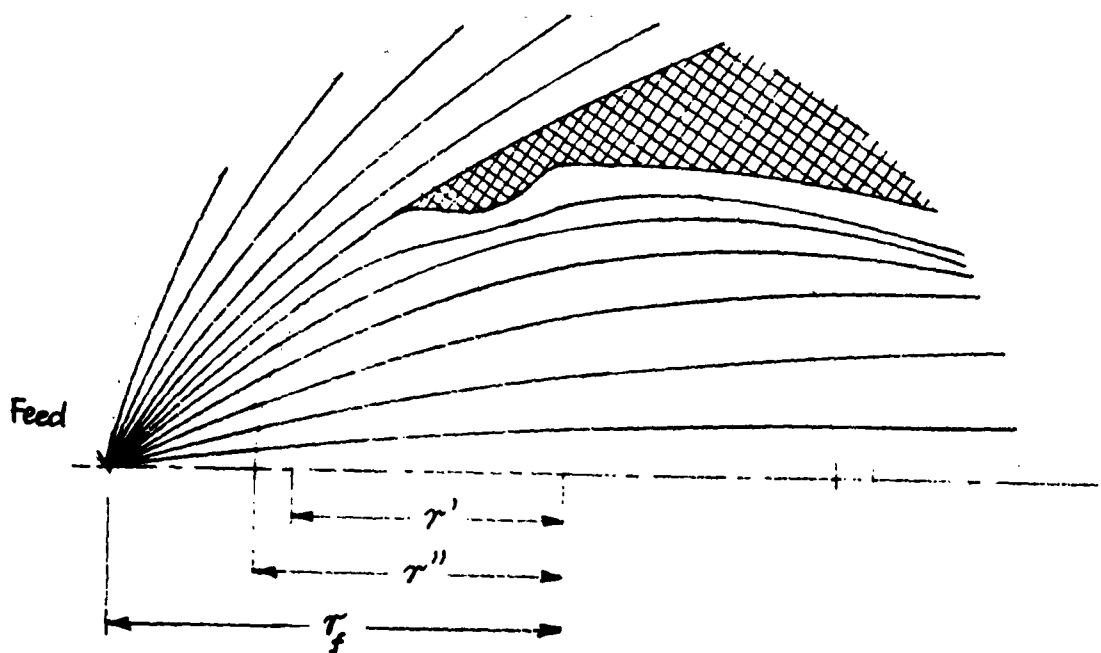


Fig. 7 Ray Paths in a Lens with an nr Distribution
as shown in Fig. 6B

Now separate from the integral in Eq. (32) the part for $r > r_a$
which is known. We find then

$$\psi_o(x) = x \int_{r_0}^{r_f} \frac{dr}{r \sqrt{n^2 r^2 - x^2}} \quad (37)$$

where

$$\psi_o(x) = \varphi_o(x) - x \int_{r_a}^{r_f} \frac{dr}{r \sqrt{n^2 r^2 - x^2}} \quad (38)$$

is a known function of x since $\phi_o(x)$ will be required to be specified such that all rays passing through the inner part $0 < r < r_a$ of the lens form a collimated beam upon leaving the lens. Obviously, $\phi_o(x)$ is therefore found from Eq. (35) by putting $\theta = 0$. Introducing Eq. (33) in Eq. (35), we find

$$\varphi_o(x) = \frac{\pi}{2} - \frac{1}{2} \operatorname{Arcsin}\left(\frac{x}{r_c}\right) - \frac{x}{2} \int_{r_f}^{r_c} \frac{dr}{r \sqrt{n^2 r^2 - x^2}} \quad (39)$$

Let us introduce this in Eq. (38). $\psi_o(x)$ is then found to be given by

$$\psi_o(x) = \frac{\pi}{2} - \frac{1}{2} \operatorname{Arcsin}\left(\frac{x}{r_c}\right) - \frac{x}{2} \int_{r_f}^{r_c} \frac{dr}{r \sqrt{n^2 r^2 - x^2}} - x \int_{r_a}^{r_f} \frac{dr}{r \sqrt{n^2 r^2 - x^2}} \quad (40)$$

The solution of Eq. (37) has been found by Kay⁴ and Morgan⁵ for the case $r_a = 1$ and $n_a r_a = 1$. The solution for this case is given by

$$n = \xi e^{\frac{2}{\pi} \int_{-\xi}^1 \frac{\psi_0(x)}{\sqrt{x^2 - \xi^2}} dx} \quad (41)$$

where ξ is a parameter defined by

$$\xi = nr \quad (42)$$

These two equations serve to determine n and r .

The solution of Eq. (37) can be deduced from Eq. (41) by transforming Eq. (37) as follows

$$\psi_0(x) = \frac{x}{n_a r_a} \int_{\frac{r_a}{\xi}}^1 \frac{d\left(\frac{r}{r_a}\right)}{\frac{r}{r_a} \sqrt{\left(\frac{n}{n_a}\right)^2 \left(\frac{r}{r_a}\right)^2 - \left(\frac{x}{n_a r_a}\right)^2}} \quad (43)$$

Obviously, this transformation normalizes both r and nr to the value 1.

Accordingly, the solution of Eq. (37) can be deduced from Eq. (41) by replacing r by $\frac{r}{r_a}$, n by $\frac{n}{n_a}$ and x by $x/n_a r_a$. Substituting also

$\xi = \xi/n_a r_a$, we find

$$n = \frac{f}{r_a} e^{\frac{n_0 r_a}{\pi} \int_f^x \frac{\psi_0(x)}{\sqrt{x^2 - f^2}} dx} \quad (44)$$

and

$$r = \frac{f}{\eta} \quad (45)$$

The method used to derive Eq. (41) restricts the solution for n_r to be a monotonic function of r .

For the evaluation of Eq. (44), we have to solve the integrals in Eq. (40). These integrals cannot be reduced to a closed form except in very special cases, among these the case where n is constant. To avoid having to integrate numerically first over r according to Eq. (40), and then over x according to Eq. (44), we shall assume that the region $r_a < r < r_c$ of the lens consists of a large number of layers, each layer with a constant index of refraction. The resulting stepped index curve can be made to approximate the actual continuous index curve as well as desired by choosing a sufficiently large number of layers. Assume that the region $r_a < r < r_f$ consists of P_1 layers with refraction indices $n_{11}, n_{12}, n_{13}, \dots, n_{1, P_1}$ and with radii $r_{11}, r_{12}, r_{13}, \dots, r_{1, P_1 + 1}$ where $r_{11} < r_{12} < \dots < r_{1, P_1 + 1}$.

We find then

$$\begin{aligned}
 x \int_{r_a}^{r_f} \frac{dr}{r \sqrt{n^2 r^2 - x^2}} &= x \sum_{p=1}^{P_1} \int_{r_{1,p}}^{r_{1,p+1}} \frac{dr}{r \sqrt{n_{1,p}^2 r^2 - x^2}} \\
 &= \sum_{p=1}^{P_1} \left[\arcsin\left(\frac{x}{n_{1,p} r_{1,p}}\right) - \arcsin\left(\frac{x}{n_{1,p} r_{1,p+1}}\right) \right]
 \end{aligned} \tag{46}$$

Assume similarly that the region $r_f < r < r_c$ consists of P_2 layers with indices $n_{21}, n_{22}, n_{23}, \dots, n_{2,P_2}$ and with radii $r_{21}, r_{22}, r_{23}, \dots, r_{2,P_2+1}$ where $r_{21} < r_{22} < r_{23} < \dots < r_{2,P_2+1}$. We find then analogously

$$x \int_{r_f}^{r_c} \frac{dr}{r \sqrt{n^2 r^2 - x^2}} = \sum_{p=1}^{P_2} \left[\arcsin\left(\frac{x}{n_{2,p} r_{2,p}}\right) - \arcsin\left(\frac{x}{n_{2,p} r_{2,p+1}}\right) \right] \tag{47}$$

Now introducing Eqs. (46) and (47) in Eq. (40), and Eq. (40) in Eq. (41), and introducing also the integral function

$$I(f, a, x) = \int_f^x \frac{\arcsin\left(\frac{x}{a}\right)}{\sqrt{x^2 - f^2}} dx, \tag{48}$$

which has been expressed as a power series in Appendix A, we find

$$n = \frac{\epsilon}{r_a} e^{\frac{2}{\pi} T(\epsilon)} \quad (49)$$

where

$$T(\epsilon) = \frac{\pi}{2} \ln \left[\frac{n_a r_a + \sqrt{n_a^2 r_a^2 - \epsilon^2}}{\epsilon} \right] - \frac{1}{2} I(\epsilon, r_c, n_a r_a)$$

$$- \sum_{p=1}^{P_1} [I(\epsilon, n_p r_p, n_a r_a) - I(\epsilon, n_p r_{p+1}, n_a r_a)]$$

$$- \frac{1}{2} \sum_{p=1}^{P_2} [I(\epsilon, n_{2p} r_{2p}, n_a r_a) - I(\epsilon, n_{2p} r_{2p+1}, n_a r_a)]$$

(50)

The numerical evaluation of the integral in Eq. (48) is discussed in Appendix A.

Equation (49) was programmed for an electronic computer. The index of refraction in this formula has been assumed to be specified in the outer part $r_a < r < r_c$ of the lens. Since the formulas derived above will be

used to design a wire-grid lens, instead we shall specify the grid-to-grid spacing, the mesh size, and the spacing between the double wires in a double-wire square mesh. The index of refraction for $r_a < r < r_c$ was then evaluated by a sub-routine program for Eq. (21). The result of the computations is a table of the index of refraction versus r according to Eq. (49). Use of Eq. (21) then gives the grid-to-grid spacing in the entire lens.

An example of the use of the computer program for synthesizing a wire-grid lens shall be presented. Assume that the lens is divided into four regions as illustrated in Fig. 8. In the region $0 < r < r_a$ the index is unknown. The mesh size used in this region is b . In the region $r_a < r < r_b$ a double-wire grid is used with linearly tapered spacing between the double wires. The double-wire grid provides a continuous "match" between a single-wire grid with mesh size b and a single-wire grid with mesh size $\frac{b}{2}$. In the regions $r_b < r < r_f$ and $r_f < r < r_c$ a single-wire grid with mesh size $\frac{b}{2}$ is used. The point source feed is placed at $r = r_f$. The values chosen in this example for r_a , r_b , r_f and r_c , and for the values of $\frac{a}{b}$ and $\frac{d}{a}$ at these radii are shown in Fig. 8. Both $\frac{a}{b}$ and $\frac{d}{a}$ are assumed to vary linearly with r (except, of course, in the region $0 < r < r_a$ where $\frac{a}{b}$ is unknown). The wire radius was chosen such that $\frac{b}{r_0} = 1000$.

The results of the synthesis for the lens example shown in Fig. 8 are plotted in Figs. 9 and 10. Figure 9 shows the nr-product and Fig. 10 the index of refraction for the entire lens. From Fig. 10 it will be observed that the index rises quite sharply near $r = r_a = 0.75$. As a result of this, the nr-curve in Fig. 9 exhibits a minimum for $r > r_a$. It was, therefore, necessary to further specify a constant index in a narrow ring $r' < r < r_a$ such that the

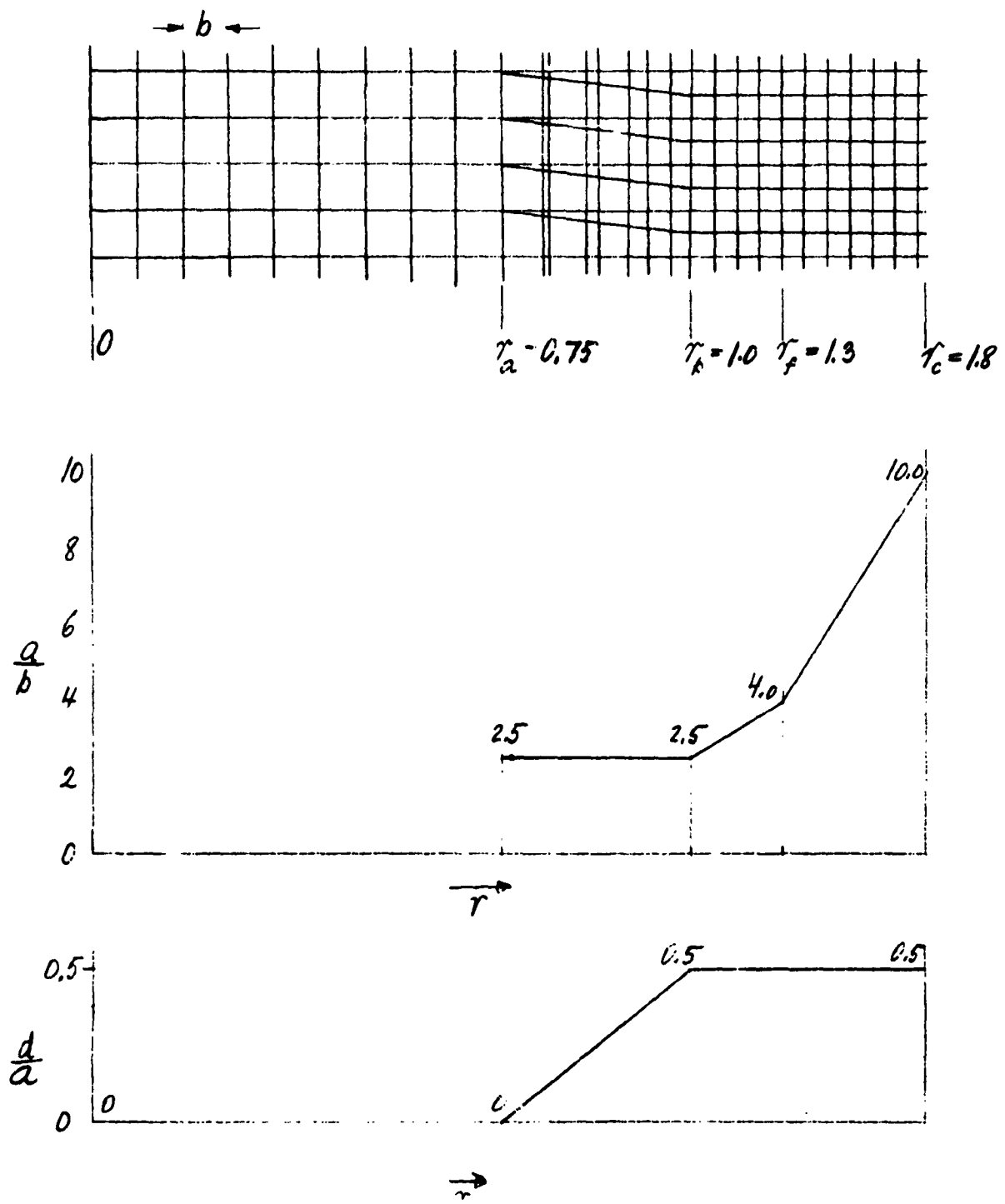


Fig. 8 Example of Circularly Symmetric Wire-Grid Lens

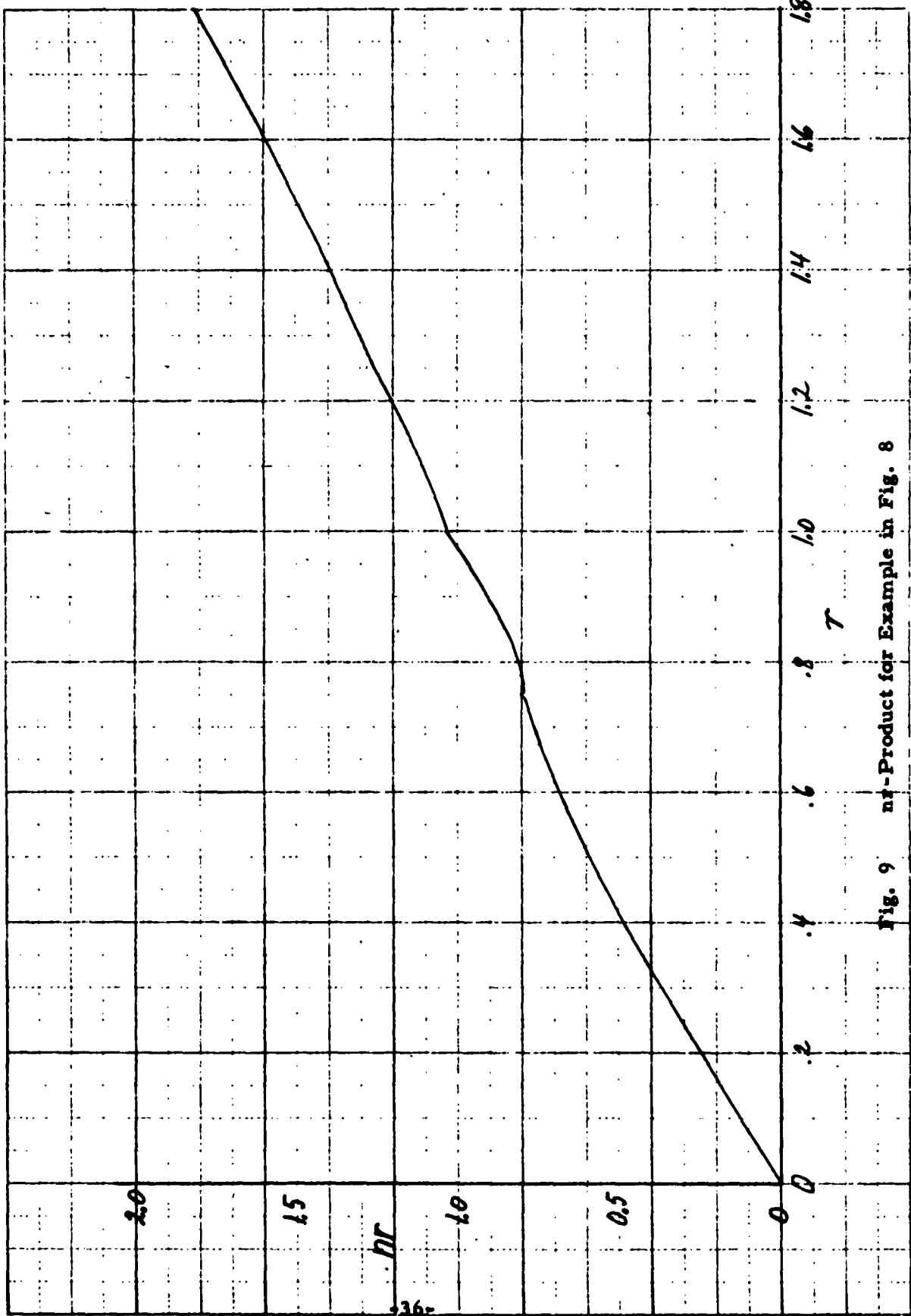
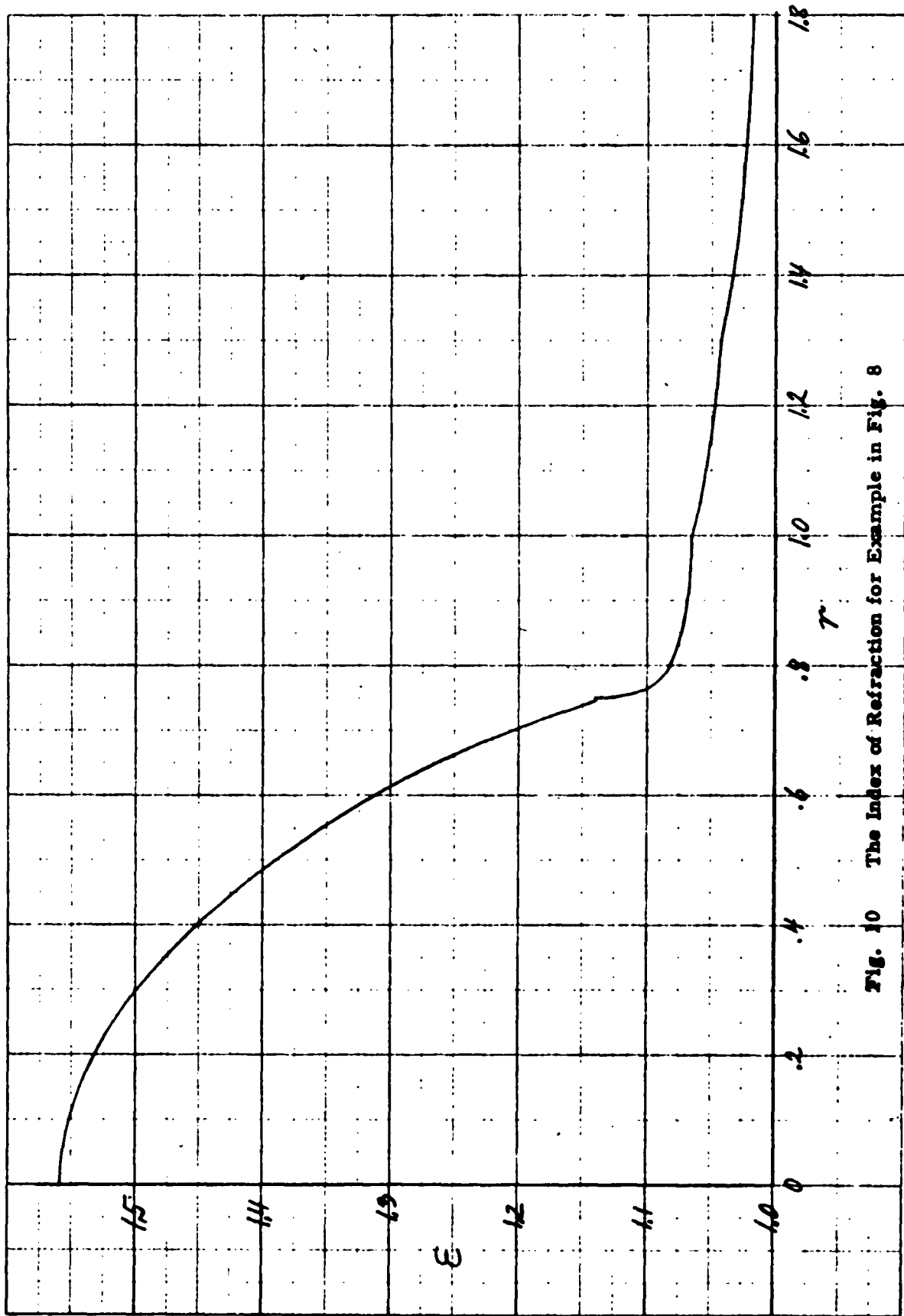


Fig. 9 $n\text{-}t$ -Product for Example in Fig. 8

Fig. 10 The Index of Refraction for Example in Fig. 8



value of nr at $r = r'$ would be the smallest value of nr for $r > r'$. This condition was satisfied for $r' = 0.745$ in the example considered. The computer is programmed to introduce the extra ring with a constant index of refraction when necessary.

The validity of the computer program for synthesizing a circularly symmetric lens was checked by synthesizing the well-known Luneburg Lens.

4. CONCLUSIONS

The investigation of a double-wire, including the special case of single-wire, square-mesh grid lens whose shape and mesh structure is specified in an outer ring of the lens, has led to a computer program which determines the grid shape in the entire lens such that the rays leaving the lens form a collimated beam in as large an aperture as possible.

APPENDIX A

For synthesizing a circularly-symmetric lens whose refractive index is specified in part of the lens, we need to evaluate the following integral

$$I(\xi, a, x) = \int_{f}^{x} \frac{\arcsin\left(\frac{x}{a}\right)}{\sqrt{x^2 - f^2}} dx$$

This integral cannot be expressed by known functions, and a numerical evaluation, when high accuracy is required, can become quite time consuming since the integrand has a singularity at the lower integration limit. Fortunately, however, the difference $I(\xi, a_2, x) - I(\xi, a_1, x)$ between two integrals with slightly different values of a enters the synthesis problem many more times than the single integral. The integral difference can be evaluated very fast and with high accuracy by expanding the integral in a power series of a .

Expanding from $a = a_0$ where

$$a_0 = \frac{a_1 + a_2}{2}$$

we find then

$$I(f, a_2, x) - I(f, a_1, x) = \frac{dI(f, a_0, x)}{da_0} (a_2 - a_1) + \frac{1}{24} \frac{d^3 I(f, a_0, x)}{da_0^3} (a_2 - a_1)^3 + \dots$$

Most often, terms of higher order than 3 in $a_2 - a_1$ can be neglected.

The first- and third-order derivatives of I can be evaluated in closed form. Differentiating I with respect to a, we find

$$\begin{aligned}\frac{dI(f, a, x)}{da} &= -\frac{1}{a} \int_f^x \frac{x dx}{\sqrt{x^2 - f^2} \sqrt{a^2 - x^2}} \\ &= -\frac{1}{2a} \left[\frac{\pi}{2} - \text{Arcsin} \left(1 - 2 \frac{x^2 - f^2}{a^2 - f^2} \right) \right]\end{aligned}$$

Differentiating this expression another two times, the following expression is found for the third-order derivative

$$\begin{aligned}\frac{d^3 I(f, a, x)}{da^3} &= \frac{1}{a^3} \left[-\frac{\pi}{2} + 2 \text{Arcsin} \left(1 - 2 \frac{x^2 - f^2}{a^2 - f^2} \right) \right. \\ &\quad \left. + \frac{a^2}{(a^2 - f^2)^2} \frac{\sqrt{a^2 - f^2}}{(a^2 - x^2)^{3/2}} (-5a^4 + 7f^2 a^2 - 6f^2 x^2 + 4a^2 x^2) \right]\end{aligned}$$

REFERENCES

1. "Investigation of Methods of Scanning the Beam of Large Antennas," Stanford Research Institute, Menlo Park, California, Final Report, Part I, Contract AF 19(604)-2240, SRI Project 2184, March 1961
2. "Investigation of a Square-Mesh Wire-Grid Modified-Luneburg Lens Antenna," Stanford Research Institute, Menlo Park, California, Scientific Report 2, Contract AF 19(604)-8059, SRI Project 3619, September 1961
3. "Investigation of Square-Mesh, Hexagonal-Mesh, and Triangular-Mesh Wire Grids for Grid-Type Lens Antenna," Stanford Research Institute, Menlo Park, California, Scientific Report 3, Contract AF 19(604)-8059, SRI Project 3619, October 1961
4. A. F. Kay, "Spherically Symmetric Lenses," IRE Trans. PGAP-7, pp. 32-38 (January 1959)
5. S. P. Morgan, "General Solution of the Luneburg Lens Problem," J. Appl. Phys. 29, pp. 1358-1368 (September 1958)

CATALOGUE FILE CARD

Rome Air Development Center, Griffiss AF Base, N.Y.
Rpt No. RADC-TDR-62-363. A STUDY OF THE WIRE-
GRID LENS, July 1962, 42pp incl illus.

Unclassified Report

This report presents a study of some problems important
in the design of a circularly symmetric type wire-grid lens.
The first problem investigated is that of a double-wire
square-mesh grid which will often be used near the rim of
the lens to keep the grid-to-grid spacing suitably small.
Design formulas for the quasi-static equivalent dielectric
constant of such grids have been derived. The validity of
these formulas was tested experimentally.
Another problem investigated is that of synthesizing the
index of refraction in a circularly symmetric lens when
the index of refraction is specified in part of the lens and

Rome Air Development Center, Griffiss AF Base, N.Y.
Rpt No. RADC-TDR-62-363. A STUDY OF THE WIRE-
GRID LENS, July 1962, 42pp incl illus.

Unclassified Report

This report presents a study of some problems important
in the design of a circularly symmetric type wire-grid lens.
The first problem investigated is that of a double-wire
square-mesh grid which will often be used near the rim of
the lens to keep the grid-to-grid spacing suitably small.
Design formulas for the quasi-static equivalent dielectric
constant of such grids have been derived. The validity of
these formulas was tested experimentally.
Another problem investigated is that of synthesizing the
index of refraction in a circularly symmetric lens when
the index of refraction is specified in part of the lens and

1. Lens antennas
2. Antennas
3. Direction finding
4. Lenses
5. Contract AF30(602)-2742

Unclassified Report

I. TRG Inc.
153 University Ave.
Palo Alto, Calif.
III. Andreasen, M. G.
Secondary Rpt. No. TRG-
West Proj. W-101, TDR
No. 1
V. In ASTIA collection

Unclassified Report

I. Lens antennas
2. Antennas
3. Direction finding
4. Lenses
5. Contract AF30(602)-2742

Unclassified Report

I. TRG Inc.
153 University Ave.
Palo Alto, Calif.
III. Andreasen, M. G.
Secondary Rpt. No. TRG-
West Proj. W-101, TDR
No. 1
V. In ASTIA collection

I. Lens antennas
2. Antennas
3. Direction finding
4. Lenses
5. Contract AF30(602)-2742

Unclassified Report

I. TRG Inc.
153 University Ave.
Palo Alto, Calif.
III. Andreasen, M. G.
Secondary Rpt. No. TRG-
West Proj. W-101, TDR
No. 1
V. In ASTIA collection

I. Lens antennas
2. Antennas
3. Direction finding
4. Lenses
5. Contract AF30(602)-2742

I. TRG Inc.
153 University Ave.
Palo Alto, Calif.
III. Andreasen, M. G.
Secondary Rpt. No. TRG-
West Proj. W-101, TDR
No. 1
V. In ASTIA collection

I. Lens antennas
2. Antennas
3. Direction finding
4. Lenses
5. Contract AF30(602)-2742

I. TRG Inc.
153 University Ave.
Palo Alto, Calif.
III. Andreasen, M. G.
Secondary Rpt. No. TRG-
West Proj. W-101, TDR
No. 1
V. In ASTIA collection

CATALOGUE FILE CARD

when it is required that the rays leaving the lens must form a collimated beam in as large an aperture as possible. Derived design formulas representing the solution of this problem are most useful for wire-grid lens designs because the grid-to-grid spacing in the outer part of the lens is often determined by mechanical rather than by electrical considerations.

when it is required that the rays leaving the lens must form a collimated beam in as large an aperture as possible. Derived design formulas representing the solution of this problem are most useful for wire-grid lens designs because the grid-to-grid spacing in the outer part of the lens is often determined by mechanical rather than by electrical considerations.

when it is required that the rays leaving the lens must form a collimated beam in as large an aperture as possible. Derived design formulas representing the solution of this problem are most useful for wire-grid lens designs because the grid-to-grid spacing in the outer part of the lens is often determined by mechanical rather than by electrical considerations.

